Available online at www.eccomasproceedia.org
Eccomas Proceedia COMPDYN (2023) 2656-2676

ECCOMAS
Proceedia

COMPDYN 2023
9th ECCOMAS Thematic Conference on
Computational Methods in Structural Dynamics and Earthquake Engineering
M. Papadrakakis, M. Fragiadakis (eds.)
Athens, Greece, 12-14 June 2023

THREE-DIMENSIONAL DISCRETE ELEMENT MODELLING OF RUBBLE MASONRY STRUCTURES FROM GEOSPATIAL DATA

Nicko Kassotakis[1,2], Vasilis Sarhosis[3] , Ajit Pillai[2], Lars Johanning[2]

[1]Imetrum
, Wraxhall, Bristol, BS48NA
e-mail: nicko.kassotakis@imetrum.com

[2]College of Engineering, Mathematics and Physical Sciences, University of Exeter
TR10 9FE, UK
e-mail: {n.kassotakis, a.pillai, l.johanning}@exeter.ac.uk

[3]School of Civil Engineering, University of Leeds
Leeds, LS2 9JT, UK
e-mail: v.sarhosis@leeds.ac.uk

Abstract

This paper presents a framework for the three-dimensional structural analysis of full-scale, geometrically irregular discontinuum structures such as rubble masonry, directly from geospatial data. A convex decomposition algorithm is adopted, whereby a watertight mesh is subdivided into so-called voronoi blocks which approximate the anisotropic nature of the rubble masonry for structural analysis. The proposed "Voronoi4DEM" framework was implemented to assess the structural stability of the southwest leaning tower of Caerphilly Castle in Wales, UK. Simulations were performed with the three-dimensional computational software 3DEC, based on the Discrete Element Method (DEM) of analysis whilst each voronoi block of the rubble masonry was represented as a rigid, distinct block while mortar joints were modelled as zero thickness interfaces which can open and close depending on the magnitude and direction of the stresses applied to them. The innovation of this framework lies in the specific geometric strategy which approximates the random nature of discontinuous materials at a block-based level (such as rubble) with sufficient accuracy, whilst vastly reducing computational times. Consequently, the approach can simulate the highly complex behaviour of rubble masonry structures with a high degree of efficiency, geometric accuracy, and automation. It is anticipated that the methodology proposed here to enable unprecedented high-level numerical modelling (block-based numerical modelling) of full-scale rubble masonry structures with, until now, unemployed techniques such as the DEM.

Keywords: Point cloud, mesh, rubble masonry, Discrete Element Method (DEM), terrestrial laser scanning, structure-from-motion photogrammetry, block-based numerical modelling

ISSN:2623-3347
Peer-review under responsibility of the organizing committee of COMPDYN 2023.
doi: 10.7712/120123.10591.21109

1 INTRODUCTION

Of the most effective and advanced approaches available for the safety assessment of our built heritage is Structural Health Monitoring (SHM). Specifically, according to Brownjohn [1], SHM regards the implementation of a scheme of monitoring a structure, through periodically spaced dynamic response measurements. Consequently, it can be employed to detect deterioration and indicated when a given structure would warrant repair, retrofit or strengthening. Making SHM ubiquitous, could safeguard our built environment from the threats of extreme loading events to an ever-changing environment (e.g., climate change, flooding etc.).

When employing SHM, two main avenues exist. The first, so-called physics-driven, is with the use of an experimental or numerical model. The second, the data-driven, is based solely on employing sensor data [2]. Effectively, in the case of a numerical model, the physics-driven approach aims to build an accurate model by calibrating the model parameters with initial sensory measurements. Then, discrepancies between model predictions and new measurements may indicate the existence of damages. On the other hand, the data-driven approach also establishes a model but is in the form of statistical representations, e.g., the probability density function. In the context of damage detection and prediction, physics-driven SHM is advantageous but extremely complicated to employ.

Due to this, high-level numerical modelling approaches are essential to protecting our built heritage. However, they are still not widely employed, remaining in the niches of research and small-scale consultation [3,4]. Specifically, when adopting the so-called block-based strategy, the geometry of the structure is depicted on a block-based level, permitting accurate depiction of failure modes and complex behaviours associated with discontinuum materials such as masonry. Of the most important obstacles in employment of the block-based strategy is the necessity for the geometrical and material properties to be represented with the highest degree of accuracy possible [5], since it permits the representation of the discontiuum structure into representative elements at a block level, according to the very nature of the material. However, for the block-based strategy to be accurate, exact geometric information is necessitated. This is often omitted, through the employment of ad-hoc or non-representative geometric models due to two major difficulties: a) the difficulty in defining each block of the structure, at a block-based level (from gaining accurate geometric data to developing the model); and b) the execution of geometrically accurate numerical models can be extremely unmanageable, owing to an unmanageably numerous block and interface numbers.

To develop geometrically accurate block-based models, there are two approaches to define geometry. The first, which is optimal where the periodicity of the material is evident (e.g., such as periodic masonry), is through defining the blocks explicitly from geometric data. Here Structure-from-Motion (SfM) photogrammetry and Terrestrial Laser Scanning (TLS) orthoimagery can be employed with traditional computer vision [6] or even machine learning algorithms [7,8]. For the case of highly heterogeneous, discontinuous materials such as rubble masonry, adobe, etc. (or any such typology of irregular internal geometry), another approach is through the so-called spatial subdivision. This can be achieved by obtaining the spatial domain occupied by the structure through a dense point cloud or mesh and subdividing accordingly. For the case of rubble masonry, this has been applied with cubic elements, so-called voxels [9-11], however with some hindrances such as high computational times, incorrect failure modes, and low geometric accuracy.

To overcome this, a novel approach of spatial subdivision, termed voronoi tessellation [12] has recently been proposed which divides the structure into voronoi blocks. This approach effectively divided the spatial domain of the analysed structure into completely interlocking cells which tessellate to form the original domain. The main advantage of the approach is that it permits the discontinuum structure's material to be represented with a high degree of geometric accuracy, whilst also representing the anisotropic nature of the material more realistically while permitting faster simulations too. Within the context of structural engineering, the voronoi tessellation approach has been successfully employed used for numerous structures and typologies such as retaining walls [13,14], masonry arch bridges, [15] masonry and adobe wallets [14,16,17], concrete [18] and even reinforced concrete structures [19]. From the above studies, it is evident that voronoi tessellation provides an optimal platform to fictitiously approximate the mathematical random nature of the discontinuum. However, until now, voronoi tessellation has not been applied in conjunction with geospatial data. On contrary, all the previous studies have been carried out with approximate or ad-hoc based geometrical models, manually designed with CAD software (such as Rhino [20]), and without highly-accurate geospatial data, such as point clouds or meshes. This presents a major limitation to the robustness and efficiency of the structural analysis.

The paper presents a framework for the 3D discrete element modelling of geometrically irregular discontinuum structures such as rubble masonry, directly from geospatial data (e.g., a mesh), employing voronoi blocks. The proposed framework was implemented on the south-west leaning tower of Caerphilly Castle located in Wales, UK. The stability of the tower was structurally assessed using the discrete element method (DEM). Within DEM, the structure can be divided into an assemblage of discrete bodies that can move independently from each other. Also, within DEM, large rotations and displacements of blocks can be allowed and new contacts and loss of existing contacts between the elements are automatically recognised and updated as the calculation progresses. This paper is organized as follows: Section 2 details the proposed "*Voronoi4DEM*" framework; Section 3 describes the case study under consideration; Section 4 presents the implementation of the proposed framework on the case study and the results obtained; and Section 5 outlines the conclusions and recommendations for future work.

2 THE PROPOSED "*VORONOI4DEM*" FRAMEWORK

In this section, the three-stage framework of the proposed automatic procedure for converting point clouds into 3D numerical models based on the DEM is described. The three-stage framework involved: Stage 1 - 3D documentation; Stage 2 - geometric model development; and Stage 3 -structural analysis. A flowchart of the proposed framework is shown in Figure 1 and a detailed description of the steps at each stage is provided below.

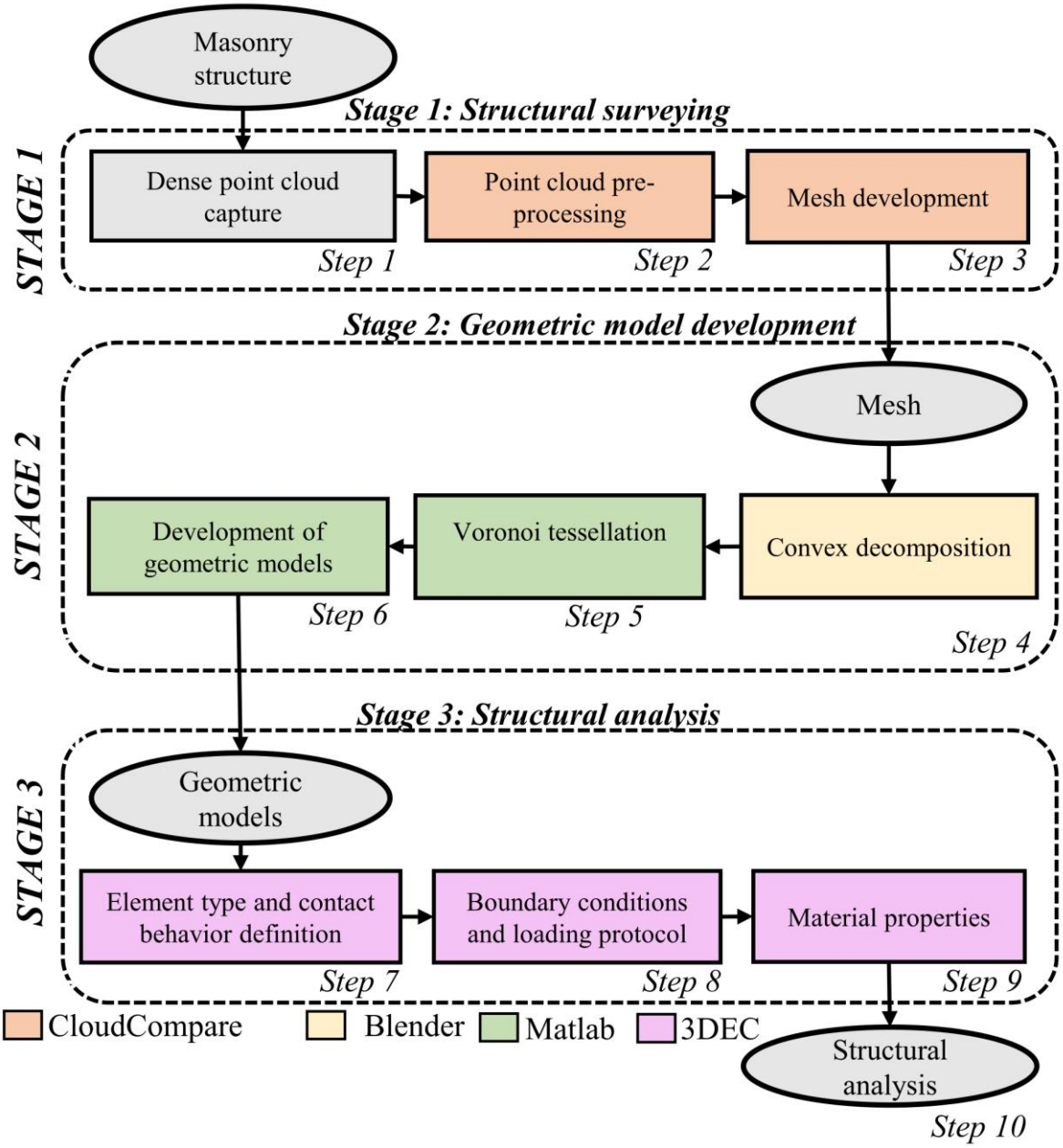

Figure 1. The "Voronoi4DEM" framework.

2.1 Structural surveying – Stage 1

The framework commences through the acquisition of highly-accurate geospatial data. Namely, through the capturing and processing of dense 3D point clouds, which will form the base of the mesh to be employed. This can be with SfM photogrammetry or Terrestrial Laser Scanning (TLS) campaign. The processes for acquiring a point cloud of a structure is well-known due to their growing popularity of the technology [4]. After, pre-processing of the point cloud can be carried out in open-source software such as *CloudCompare* [21]. This step is important to merge various point clouds composing the entirety of the structure. It also permits the cleaning and cropping of the point cloud to retain the structure subject to structural analysis inside the point cloud, solely. Finally, from the pre-processed point cloud, a watertight mesh can be constructed using the Poisson surface reconstruction algorithm. This study employed a plugin within *CloudCompare* based on the well-known Poisson reconstruction algorithm [22].

An indicative mesh of a rubble structure (Figure 2a) employed for the case of demonstrating the methodology is demonstrated in Figure 2b. The settings employed for mesh construction were an octree (the term octree refers to the partitioning of the 3D space by recursively subdividing it into eight octants-octrees, which are a 3D analogy of quadtrees), depth of 12, samples per node equal to 1.5, full depth equal to 5, the point weight equal to 4.0 and the boundary set as free.

2.2 Geometric model development – Stage 2

Firstly, based on the watertight mesh from the Poisson reconstruction, a convex decomposition algorithm was employed to break the initial watertight mesh into subdomains, each one a convex mesh, demonstrated in Figure 2c. Here it is to be noted that for a given mesh S, convex decomposition means partitioning it into a minimal set of convex sub-surfaces [23]. To carry out this, the software *Blender* [24] was employed with the following *V-HACD* addon [25]. Settings employed were a voxel resolution equal to 100,000, clipping depth equal to 20, maximum concavity equal to 0.0025, plane down-sampling equal to 4, and convex-hull down-sampling equal to 4. Also, the approximate decomposition mode was employed with alpha equal to 0.05, beta equal to 0.05, gamma equal to 0.0125, maximum vertices per convex hull equal to 32, and maximum volume of convex hull equal to 0.001 m^3. After, a key step of the procedure was carried out, which concerned voronoi tessellation. Firstly, the definition of the centroids of the voronoi blocks was carried out. This was through filling the internal of the convex meshes with points, herein termed the artificial internal point cloud, as shown in Figure 2d. This was achieved within a *Matlab* [26] script by merely assigning points to the interior of the geometrical domain of each convex hull, with a randomization algorithm. At this point, the resolution of the voronoi tessellation was selected based on the density of the artificial internal point cloud assigned. Here, the voronoi tessellation resolution is defined based on a predefined ratio of approximate volumetric subdivision of the initial convex hull. For instance, the voronoi resolution of the model in Figure 2e is of a voronoi block with a volume of approximately 1 m^3. To finish the voronoi tessellation process, an algorithm was employed to convert each convex hull and its respective artificial internal point cloud, into a sum of voronoi blocks, however in a mesh format (e.g., .obj files). This was through employing an existent *Matlab* script [27] for automated 3D voronoi tessellation, automatically, as shown in Figure 2e. Finally, based on the outputs of the latter algorithm, the geometric model development was carried out, which sought to convert the voronois block from mesh format to one compatible with the structural analysis software. This resulted in a block-based model study compatible with the DEM numerical modelling software 3DEC [28]. Specifically, each block of the geometric model was defined as a multi-faced polyhedron, as shown in Figure 2f. It is noteworthy that the same geometric models generated can also be for other block-based numerical methods such as the Finite Element Method (FEM) [29] and Applied Element Method (AEM) [30].

(a)

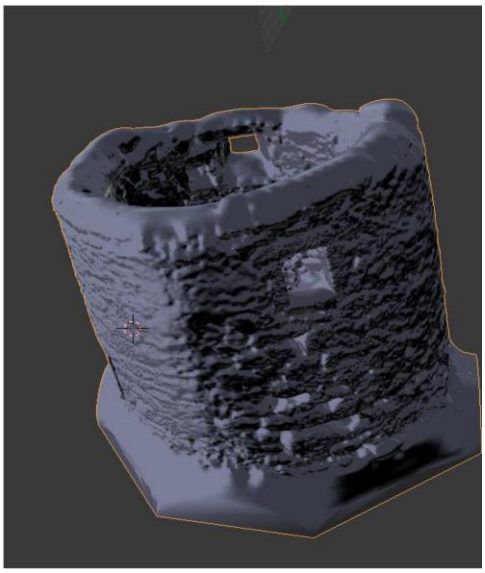

(b)

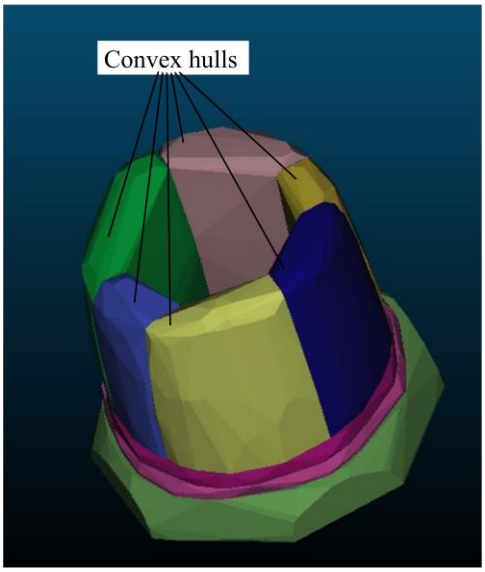
Convex hulls

(c)

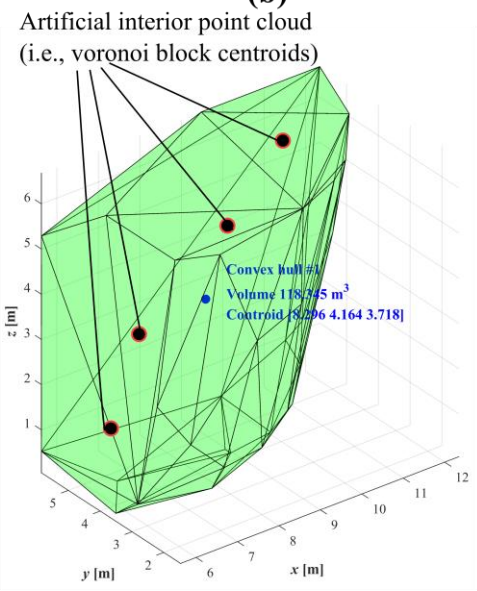
Artificial interior point cloud
(i.e., voronoi block centroids)
Convex hull #1
Volume 118.345 m3
Centroid [8.296 4.164 3.718]
z [m]
y [m]
x [m]

(d)

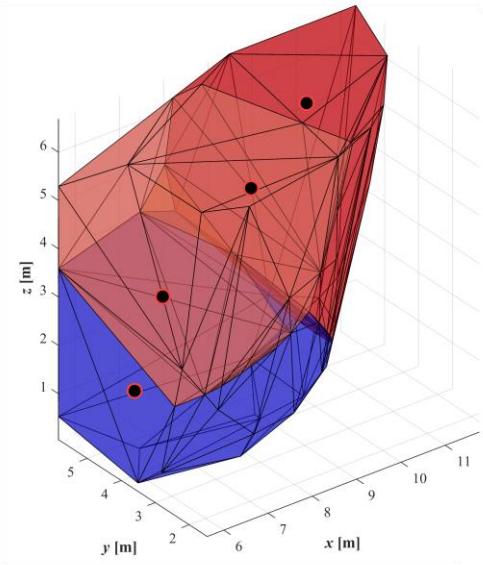
z [m]
y [m]
x [m]

(e)

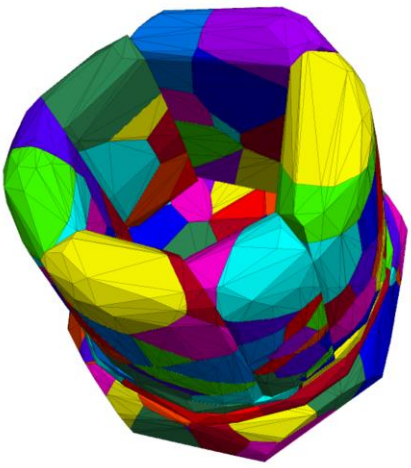

(f)

Figure 2: Indicative application of methodology on masonry tower for illustrative purposes: (a) view of the tower; (b) watertight mesh of tower; (c) convex decomposition process; (d) geometric representation of convex hull, with artificial interior point cloud: (e) geometric representation of voronoi tessellation of convex hull; and (f) whole geometric model in 3DEC.

2.3 Structural analysis with the discrete element method – Stage 3

DEM is an approach that has been widely used to simulate the static and dynamic behaviour of blocky structures. Within DEM, masonry units (i.e., blocks) are represented as rigid or deformable blocks, which may form any arbitrary geometry. Interactions between blocks are governed by appropriate stress-displacement constitutive laws at point contacts at the edges of the blocks [28]. The motion of the blocks is simulated throughout a series of small but finite time steps, numerically integrating the Newtonian equations of motion. Contacts in blocks can be face-to-face, vertex-to-face or edge-to-edge type. The seldom case of edge-to-edge is shown in Figure 3a. Finite displacements of the discrete bodies and rotations are allowed, which includes the complete detachment of blocks and new contact generation as the calculation proceeds. Forces are considered as linear functions of the actual penetration in the shear and normal directions [31].

Figure 3b-c shows the adopted Mohr-Coulomb joint constitutive model implemented in 3DEC. The inelastic material properties used within these models were the joint cohesive strength (c), the joint tensile strength (T), and the joint friction angle (φ). According to the adopted joint constitutive model, the structure's behaviour is governed by the joint normal and shear stiffnesses, K_n and K_s in the normal and shear elastic range accordingly.

In the model, the tensile normal force is limited to T_{max} and the shear force is limited to F^s_{max} ; see equations (1) and (2); where T is joint tensile strength, A_c is the sub-contact area, c is joint cohesive strength and φ is the joint friction angle.

$$T_{max} = -T \times A_c \tag{1}$$

$$F^s_{max} = c \times A_c + F^n \times tan\,\varphi \tag{2}$$

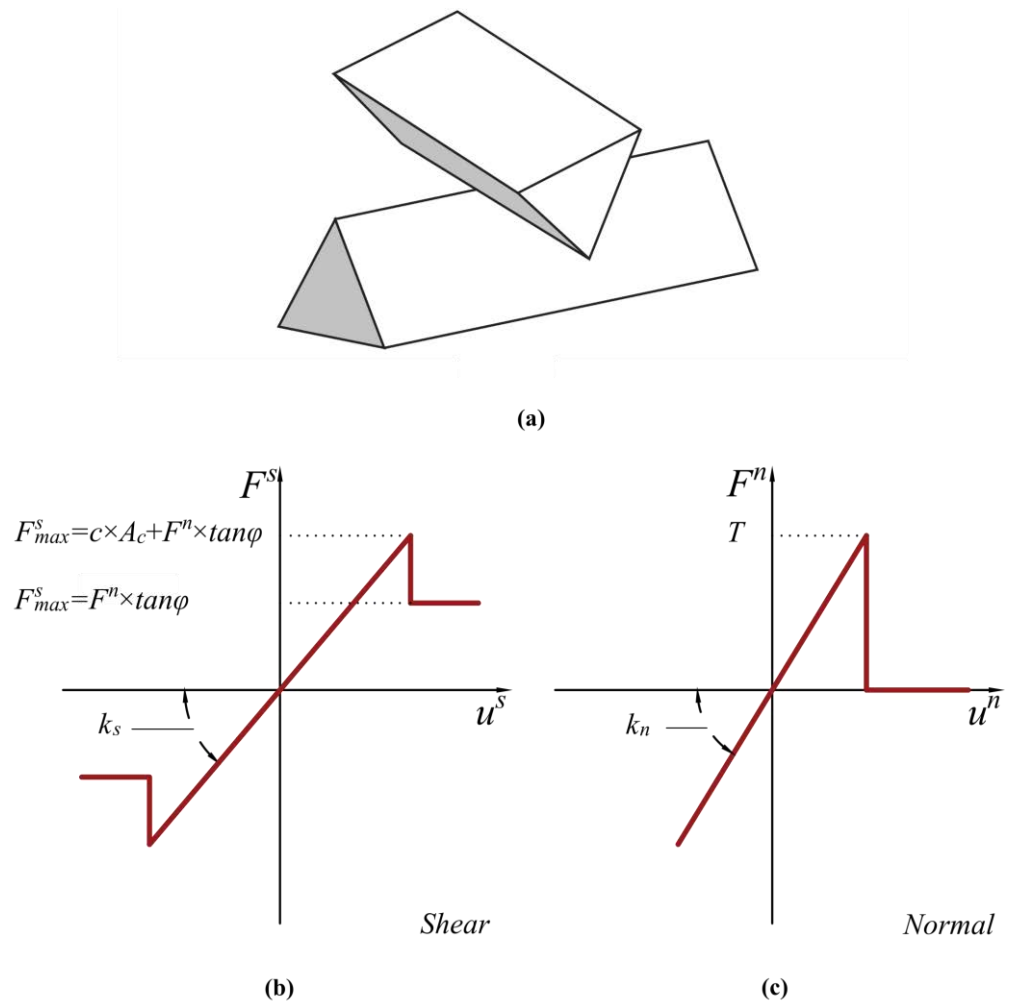

Figure 3. Contact between two blocks: the seldom edge-to-edge type contact (a) [28]. Force-displacement relationship of the adopted joint constitutive model for: (b) shear; and (c) normal direction.

Regarding boundary conditions, the approach employed is to consider the base of the structure fixed from a certain point and onwards. This is an idealisation of real conditions, where soil presents an amount of movement. However, it is a necessity in the absence of real-world sensing data regarding foundations. To carry this out, a zero velocity was applied to the specific zone of the model which is considered fixed. It is to be noted that the employment of the framework in conjunction with sensory data from a structure, as in [32] could establish a better approximation of boundary conditions based upon a model updating scheme. After boundary conditions, material properties can be applied. When employing the block-based approach, (such as in general for periodic masonry) structures are usually explicitly modelled as masonry units and are represented as an assemblage of distinct blocks separated by zero-thickness interfaces at each mortar joint. In this case, defining material properties, is a relatively straightforward procedure, see [33,34]. However, in this study, in the absence of the actual knowledge of the rubble masonry's geometrical layout (i.e., construction pattern), material properties of the voronoi blocks must be employed which can mathematically approximate the rubble masonry. To achieve this, a homogenization procedure such as the one proposed in [35] can be used to obtain the material properties which characterise the mechanical interaction between blocks. Additionally, the models can be calibrated against experimental data on rubble structures, as in [36]. After material properties, the loading protocol can be assigned. This can vary according to the structure, as will be demonstrated in the forthcoming paragraphs.

3 THE SOUTHWEST LEANING TOWER OF CAERPHILLY CASTLE

The southwest leaning tower of the Caerphilly tower located in South Wales, UK (Figure 4a) and was employed to evaluate the proposed framework. Caerphilly is one of the largest castles in Europe [37] and the second largest in the UK [38]. It is believed to be leaning because of the lack of foundation strength and stiffness which was induced by dewatering in the 18th Century. The tower stands 17 m tall and 9 m in diameter, with a current inclination equal to circa 10 degrees off vertical.

The employment of the tower is of particular interest to this study, since it highlights the proposed framework's potential in contrast with other approaches. For instance, several analytical approaches exist to investigate the safety of leaning towers. However, such approaches cannot be applied to irregular geometries (e.g., highly irregular in shape, with openings, voids, and a non-rectangular base). Moreover, many computational methods such FEM and Limit Analysis also exist and have been applied to leaning towers with complex geometry [39,40]. However, the former cannot always accurately describe the discontinuous nature of masonry [41], while the latter can, but still relies upon simplified assumptions [40] and is not able to provide information about the in-service condition of the structure under consideration. This proposed approach overcomes both previous difficulties.

4 APPLICATION OF THE PROPOSED FRAMEWORK IN THE CASE STUDY

Various geometric models of the Caerphilly tower have been developed in this study, of which one was employed for structural analysis. Though another three models with varying voronoi block sizes were also developed (as demonstrated in Figure 6), structural analysis was not undertaken. This was considered out of the scope of the current investigation, which was to merely demonstrate the framework in quantitatively assessing the three-dimensional mechanical behaviour of highly complex behaviour of rubble masonry structures.

4.1 Structural surveying

Figure 4b shows the dense point cloud obtained from a survey to document the structural health condition of the tower in 2014 [37]. In this instance, a FARO Focus 3D ×130 terrestrial laser scanner was used to acquire 27 scans of the entire castle. The main challenges related to the 3D documentation of the castle were the foreign objects (e.g., scaffolding, non-structural artefacts, and statues); and pedestrians since the site is a significant tourist attraction. Twelve spherical targets were used to complete the registration process for the entire survey.

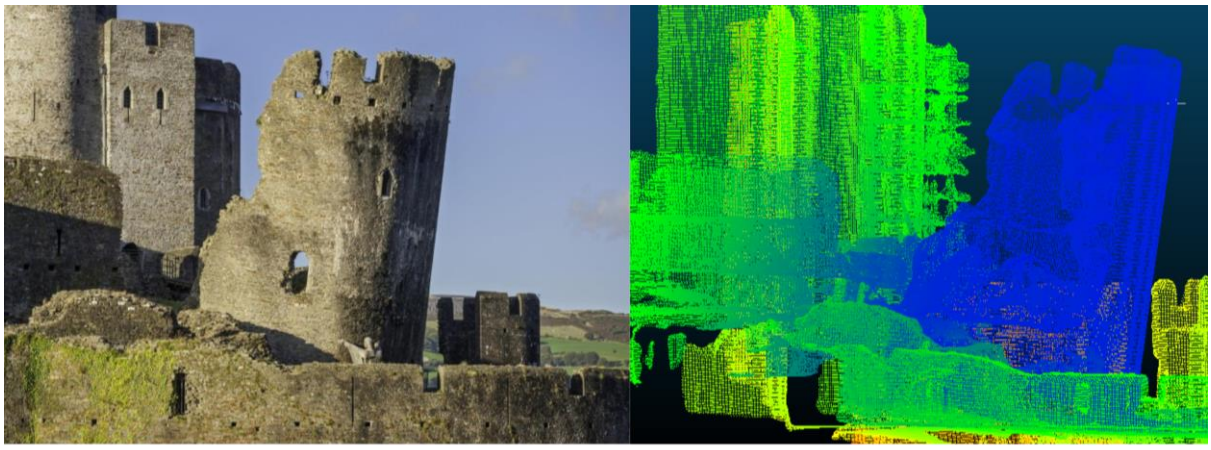

(a) **(b)**

Figure 4. Caerphilly Castle [38]. View of the face of the southeast leaning tower: (a) photograph; and (b) point cloud.

4.2 Geometric model development

In Figure 5, the application of the framework for geometric model development is demonstrated. Specifically, parting from the original watertight mesh of Figure 5a, the convex decomposition was carried out, leading to a sum of twenty-one convex meshes, as shown in Figure 5b. After, Figure 5c-d show the procedure of developing voronoi tessellation from an indicative convex hull, with the voronoi blocks indicated. Finally, Figure 5e-f show the voronoi blocks in the final format of the numerical modelling software, ready for structural analysis. In Figure 6, are three geometric models developed with approximate voronoi block volumes of approximately 5, 3 and 1 m^3. For the simulations in the following paragraphs, only the geometric model with a coarse resolution of 5 m^3 was employed. This was to merely demonstrate the framework in quantitatively assessing the three-dimensional mechanical behaviour of highly complex behaviour of rubble masonry structures.

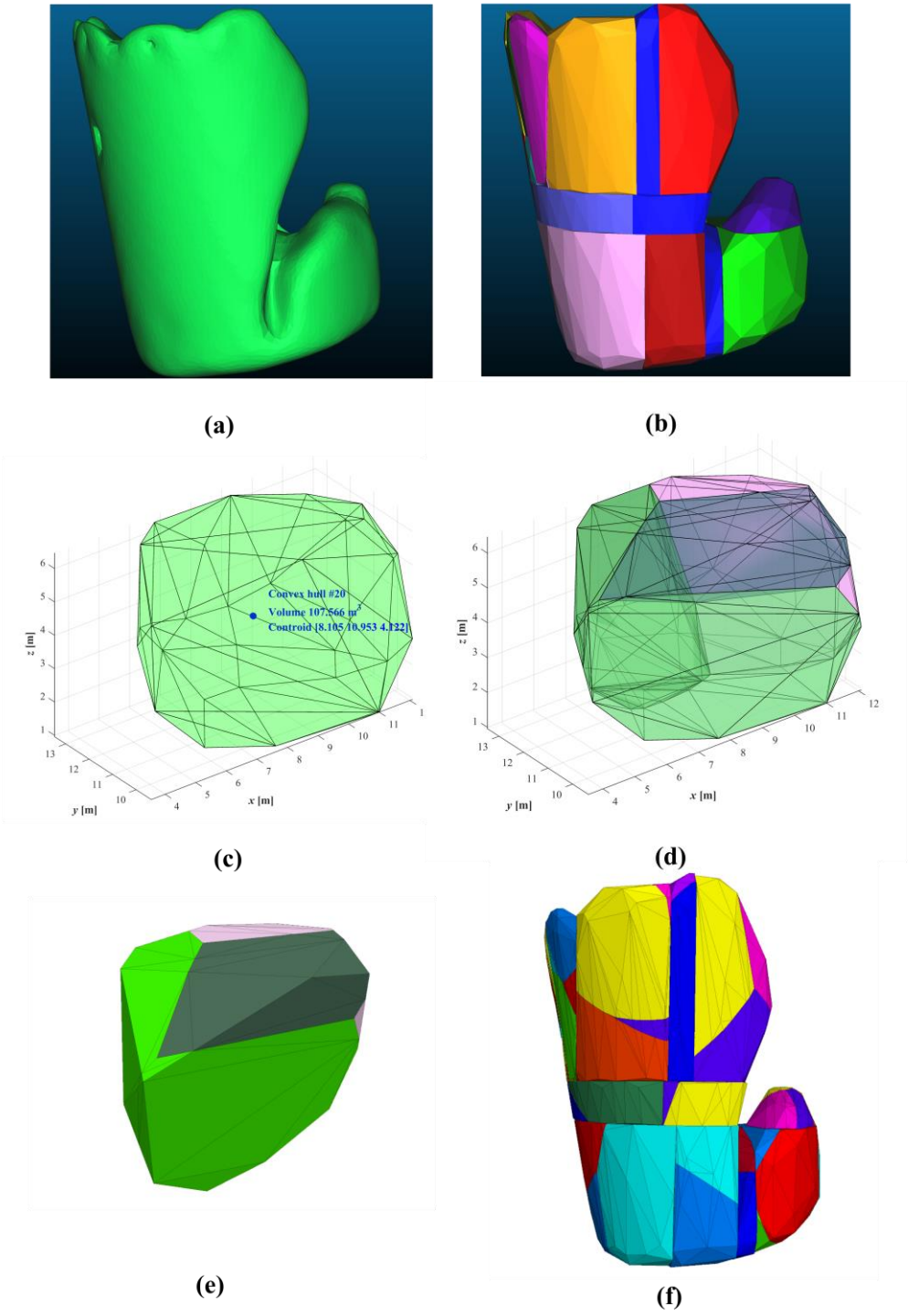

Figure 5. Geometric model development on Caerphilly tower: (a) watertight mesh; (b) convex decomposition process; (c) geometric representation of convex hull: (d) geometric representation of voronoi tessellation of convex hull; (e) voronoi tessellation of convex hull in 3DEC; and (f) whole geometric model in 3DEC.

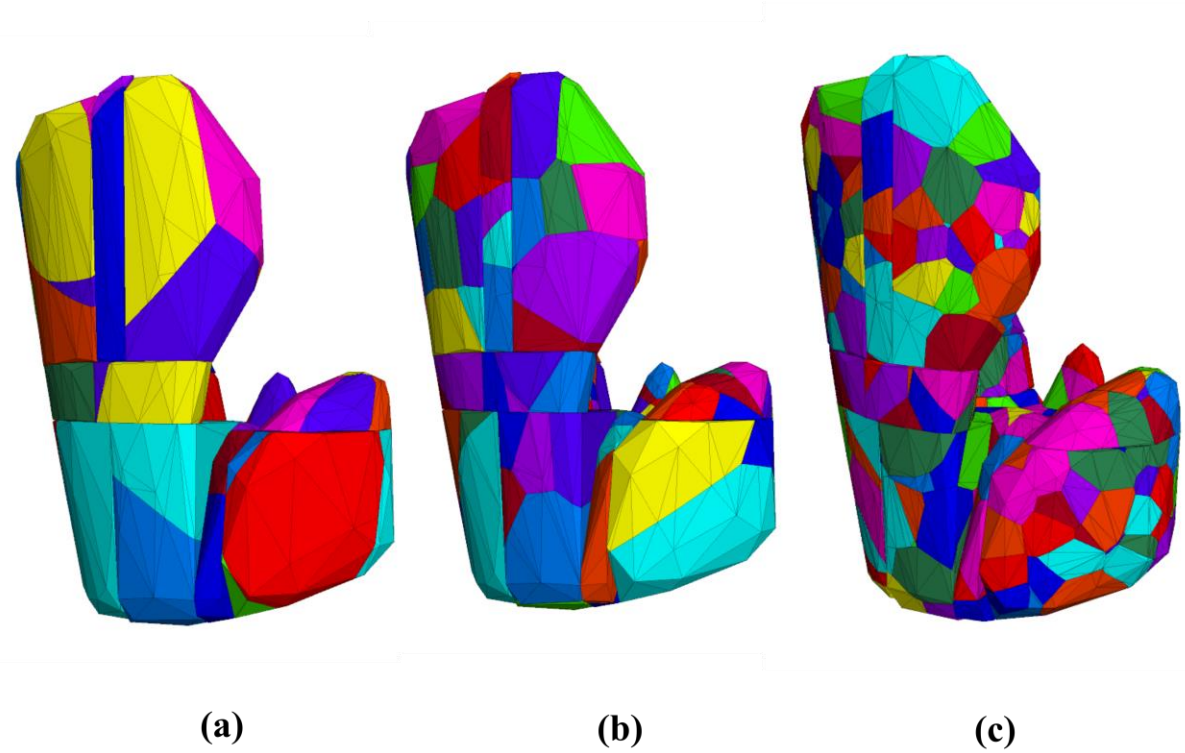

Figure 6: Various geometric models developed: (a) low-resolution 5 m^3; (b) medium resolution 3 m^3; and (c) high-resolution 1 m^3 approximate voronoi block volumes.

4.3 Structural analysis

To carry out structural analysis, parting from the geometric model, firstly indicative material properties were assigned to the numerical model. These were obtained from a previous numerical study [11] on the tower and deemed suitable for examining the current framework employing voronoi blocks, as listed in Table 1. After, the boundary conditions were assigned, according to Figure 7a-c. Specifically, the bottom of the tower was considered fixed at a height of approximately 1 m from the bottom extremity of the tower. As aforementioned, this was through applying a zero velocity at the blocks in this vicinity. Finally, after the boundary conditions, a loading protocol was defined in the same tilt-table fashion as a previous study [11]. In the numerical model, a tilt plane analysis was performed to quantify the maximum theoretical inclination angle (θ_t) of the tower, if it were situated on a tilted plane. This value was effectively the measure of the tower's structural capacity. The inclination angle was estimated by applying a horizontal acceleration (g_h) equal to $\lambda_h \times$ g, see equation (3) and altering the vertical acceleration of gravity from g to g_{vz} , equal to $\lambda_v \times$ g, see equation (4). The horizontal and vertical inclination angle multipliers λ_h and λ_v were obtained from the equations (3) and (4). Figure 8a shows a view of the tower with the gravitational acceleration components annotated.

$$\lambda_h = \sin(\theta_t) \tag{3}$$

$$\lambda_v = \cos(\theta_t) \tag{4}$$

Figure 8b shows the plan of the tower base and the azimuth (ψ) of inclination (i.e., horizontal direction in which the inclination takes place). In the numerical model, 3D loading due to the theoretical inclination was achieved by assigning gravitational acceleration components as per equations (5) to (7).

$$g_{hx} = g \cdot \lambda_h \cdot \cos\psi \tag{5}$$

$$g_{hy} = g \cdot \lambda_h \cdot \sin\psi \tag{6}$$

$$g_{vz} = g \cdot \lambda_v \tag{7}$$

In particular, equations (5), (6) and (7) describe the x-axis horizontal component, y-axis horizontal component, and vertical component of gravity, respectively (as shown in Figure 8a-b). So, for any given azimuth of inclination (ψ), the theoretical inclination angle (θ_t) is proportional to the horizontal component of gravity applied to the structure. The resulting destabilization is common with that of a tilt table, parallel to the azimuth of inclination (ψ).

Starting from a value of θ_t equal to 0 (no inclination), the theoretical inclination angle θ_t was increased incrementally. During the simulation, the inclination angle multiplier λ_h (corresponding to θ_t) was recorded. The critical inclination angle $\lambda_{h,max}$ was employed to assess the load-bearing capacity of the structure, equal to the inclination angle multiplier at which the structure could not arrive at equilibrium at the end of a given loading cycle. This was calculated by monitoring both the total unbalanced force of the model and the so-called inclination angle multiplier-displacement curves of strategically selected monitored points. The unbalanced force [28] is a metric employed to evaluate the mechanical equilibrium state of the model (and subsequent occurrence of the joint slip or plastic flow of the blocks), during structural analysis. Equilibrium of the model is achieved when either the net nodal force vectors at each block centroid or gridpoint are equal to zero and this is monitored in form of: a) the maximum nodal force vector termed the "unbalanced" or "out-of-balance" force; or alternatively b) the ratio of the unbalanced force towards the representative forces of the system, termed "unbalanced force ratio". During the structural analysis of this investigation, an unbalanced force ratio equal to 1e-4 was employed. This means that during the loading, increments were added if the unbalanced force ratio was smaller than or equal to 1e-4.

It's also important to note that at this point, the monitored points at Points A, B and C, shown in Figure 8c were strategically selected, being situated: a) on the azimuth of theoretical rotation of ψ equal to 60°; and b) at various heights (top, mid-height and bottom). This selection of the monitored points ensured reliable information about the structure's behaviour was provided for global and local failure, in the principal direction of loading. It's noteworthy that two indices relating to the structural capacity were recorded, the inclination angle multiplier at the first crack $\lambda_{h,1}$, and the critical inclination angle multiplier $\lambda_{h,max}$ (at failure). Additionally, the horizontal displacements at the first crack $U^A_{h,1}$, $U^B_{h,1}$ and $U^C_{h,1}$ and the critical horizontal displacements $U^A_{h,max}$, $U^B_{h,max}$ and $U^C_{h,max}$ of the monitored points A, B and C were also employed as a metric for quantifying the tower's deformation capacity. Finally, the structural stiffness was also calculated as the ratio of the inclination angle at the first crack towards the respective horizontal displacement at the first crack.

Parameter	Symbol	Unit	Model Values
Joint Normal Stiffness	K_n	GPa/m	20
Joint Shear Stiffness	K_s	GPa/m	15
Joint Cohesive Strength	C	MPa	0.25
Joint Tensile Strength	*T*	MPa	0.25
Joint Friction	φ	°	25

Table 1: Mechanical properties of the zero-thickness interface in the numerical models.

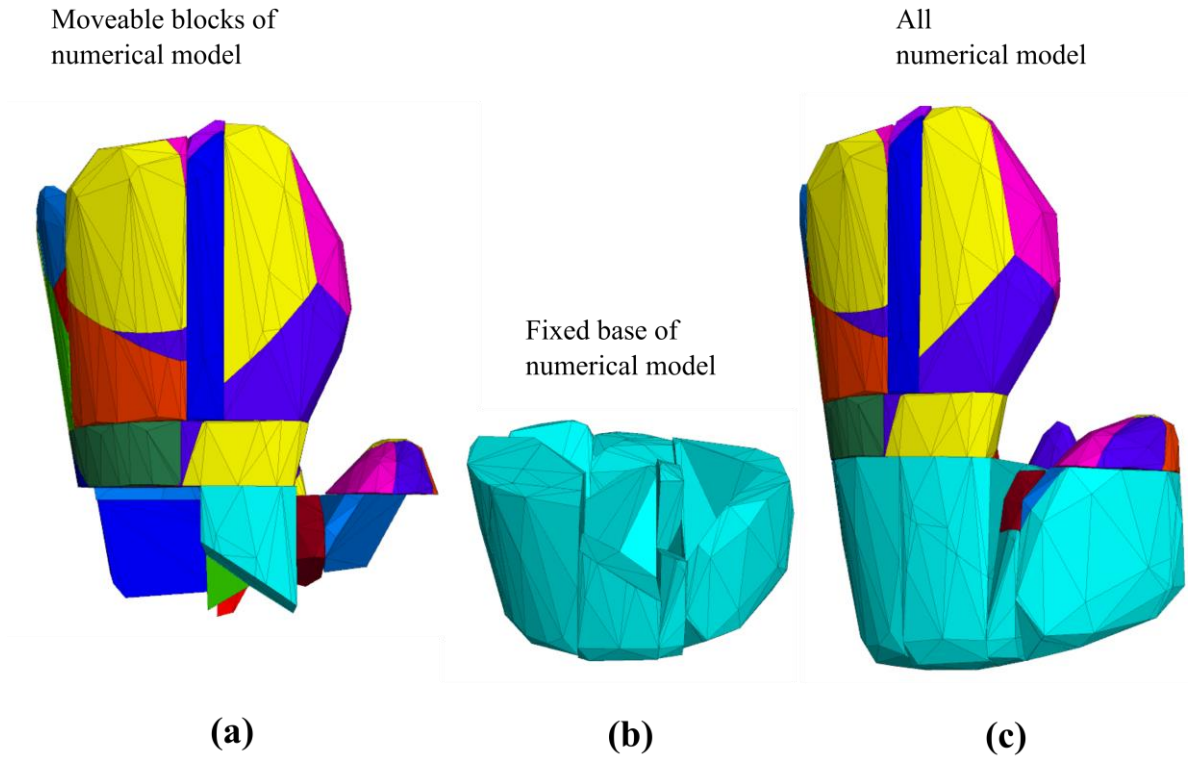

Figure 7. View of the numerical model of the tower developed using DEM: (a) Moveable blocks of the numerical model; (b) fixed base of the numerical model; and (c) all numerical models.

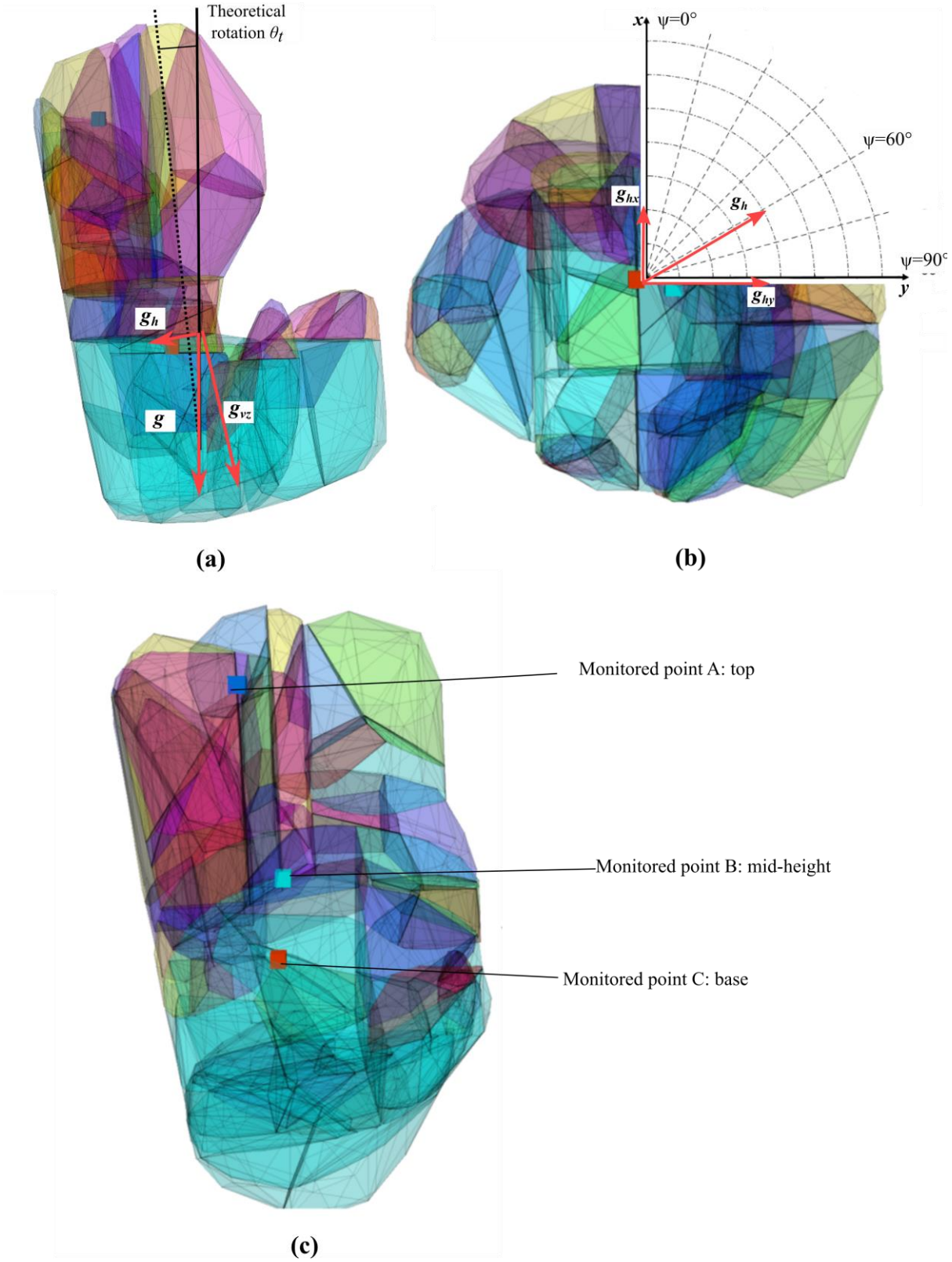

Figure 8. Loading protocol. The tower with gravitational acceleration components annotated (the dark red vertices denote the gravitational acceleration components for a theoretical inclination angle of θ_t): (a) view; (b) plan of the tower base with the azimuth of inclination (ψ); and (c) monitored points A, B and C at the top, mid-height and base of the tower.

In Figure 9a-d, are the results of the numerical analyses. Specifically, Figure 9a demonstrates the inclination angles at the first crack (considered 0.5 mm movement of blocks) and failure (considered 7.5 mm movement of blocks). Figure 9b demonstrates the stiffness, and Figure 9c-d demonstrate the tower's deformation capacity at the first crack and failure, for the various monitored points. From Figure 9, there is a good agreement with previous investigations on the tower [11], the tower has its lowest structural capacity suggesting that for 60° azimuth of inclination, the tower is weakest. It is also to be noted that simulation was carried out in a manageable computational time of circa 10 minutes for a geometric model with 86 blocks, 345 contacts. This is promising, showing the framework capable of producing valuable results, in a fraction of the time, block and contacts number of the previous simulations [11].

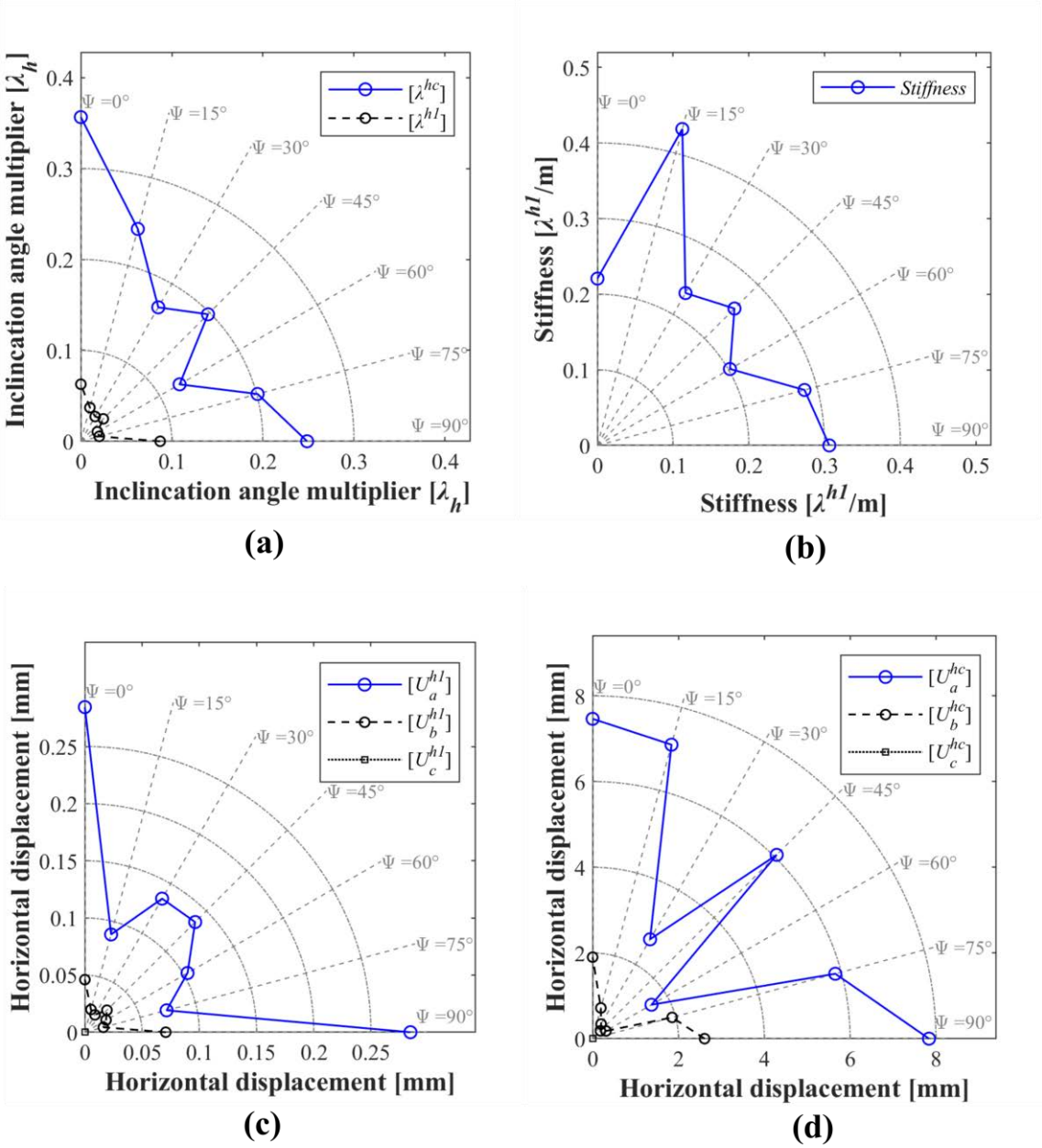

Figure 9: Structural capacity indices of the tower: (a) inclination angle multipliers at first crack and failure; and (b) the stiffness of the tower. The tower's deformation capacity at: (c) first crack; and (d) failure.

In Figure 10a, the load-displacement curve is demonstrated, for 60° azimuth of inclination. In Figure 10b-c, the displacement contours of the tower are displayed for the first crack and failure of the tower. Finally, in Figure 10d, the failure mode of the tower is displayed (with a scale factor equal to 100) is displayed. From Figure 10, there is good agreement with numerous previous studies on the stability of the tower [11] demonstrating the potential to quantitatively assess the three-dimensional mechanical behaviour of complex in geometry, rubble masonry structures such as towers.

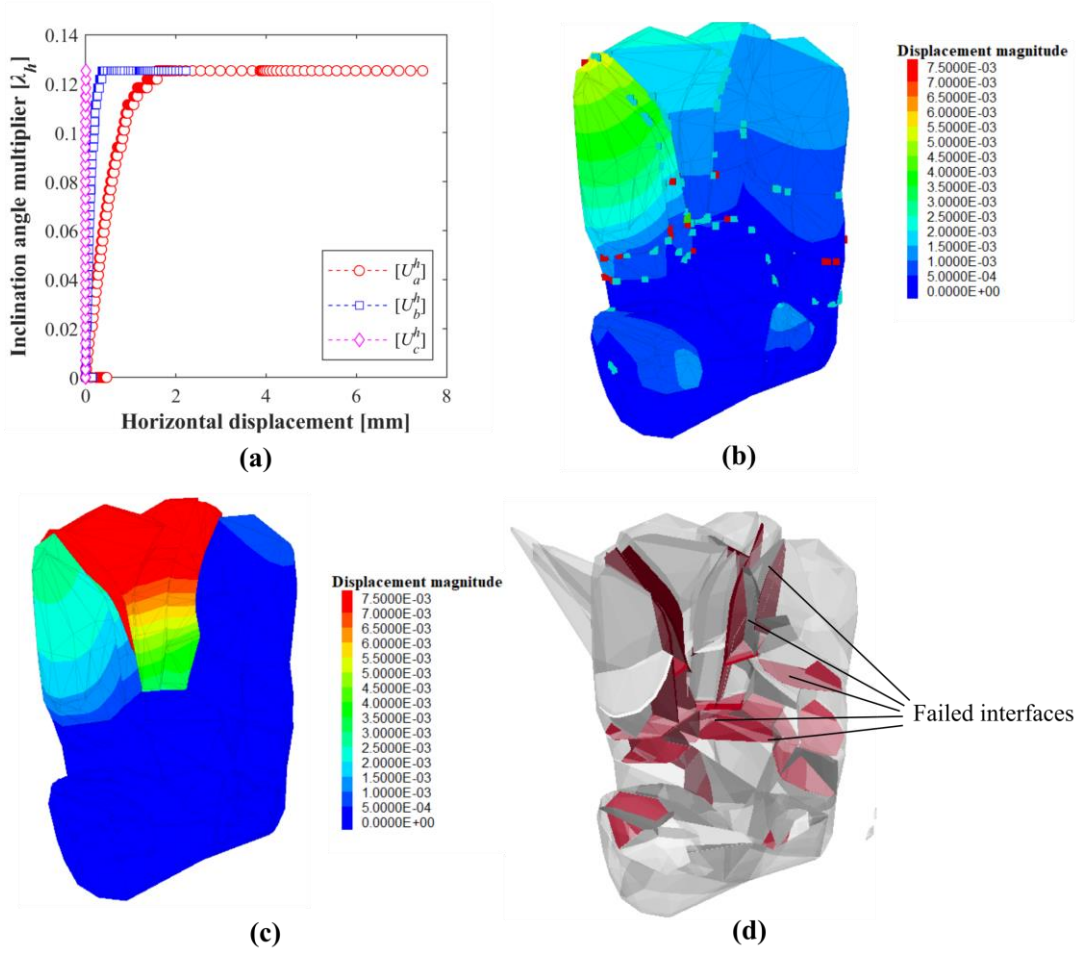

Figure 10: Failure mode of the tower: (a) inclination angle multiplier-displacement curves for 60° azimuth of inclination; (b) displacement contours at the first crack (considered 0.5 mm movement of blocks), where the blue markers denote joint tensile failure and the red marker slipped contacts; (c) displacement contours at failure (considered 7.5 mm movement of blocks); and (d) the failure mode of the tower including failed interfaces (dark red).

5 CONCLUSIONS

This paper presented a framework for the three-dimensional structural analysis of full-scale, geometrically irregular rubble masonry structures from meshes generated from Structure-from-Motion photogrammetry or terrestrial laser scanning. A convex decomposition algorithm is adopted, whereby a watertight mesh is down-sampled into so-called voronoi elements which approximate the anisotropic nature of the rubble masonry for structural analysis. The proposed "*Voronoi4DEM*" framework was implemented to assess the structural stability of the southwest leaning tower of Caerphilly Castle in Wales, UK. Simulations were performed with the three-dimensional computational software 3DEC, based on the DEM of analysis whilst each voronoi block of the rubble masonry was represented as a rigid, distinct block while mortar joints were modelled as zero thickness interfaces which can open and close depending on the magnitude and direction of the stresses applied to them. The innovation of this framework was in the specific geometric strategy which approximates the random nature of discontinuous materials at a block-based level (such as rubble) with a high accuracy whilst vastly reducing computational times. Consequently, the approach could simulate the highly complex behaviour of rubble masonry structures with a high degree of efficiency, geometric accuracy, and automation.

From the application of the framework, the potential of the proposed "*Voronoi2DEM*" framework has been demonstrated to quantitatively assess the three-dimensional mechanical behaviour of complex geometry rubble masonry structures. For the specific case study investigated herein (i.e., the Caerphilly tower), for a course voronoi block size (approximately equal to 5 m^3), structural analysis was carried out in a manageable computational time of circa 10 minutes for a geometric model with 86 blocks, 345 contacts. This is promising, showing the framework capable of producing valuable results, in a fraction of the time, block and contacts number of the previous simulations [11].

The above findings suggest that with the proposed procedure, it is possible to perform unprecedented structural analyses of discontinuum structures employing high-level structural analysis methods such as the DEM in a manageable time. Since voronoi tessellation has been successfully employed with other structural typologies such as concrete [18] and even reinforced concrete structures [19], this study opens the door to block-based analysis of other structures apart from rubble masonry.

To increase the robustness of the structural analysis of the proposed approach, a future study should be carried out with various resolutions of voronoi blocks. Additionally, another study should assess the influence of material properties, and intend to calibrate models against experimental data. Another major advancement would be to employ this framework in conjunction with sensory data from actual structures. Instead of conventional contact-based sensors, this could be achieved with non-contact sensing techniques such as Digital Image Correlation [42-44]. This would provide an updated model-driven SHM approach based on modal frequencies in the spirit of [32], however with a state-of-the-art block-based model.

6 ACKNOWLEDGEMENTS

The work presented in this paper has been financially supported by an *Innovate UK* Knowledge Transfer Partnership (KTP) project (number: 1026781). The authors also gratefully acknowledge Dr Oriel Priezman for providing the point cloud of the southwest tower of Caerphilly Castle.

REFERENCES

[1] J. Brownjohn, Structural health monitoring of civil infrastructure, Philosophical transactions. Series A, Mathematical, physical, and engineering sciences 365 (2007), pp. 589-622, DOI: 10.1098/rsta.2006.1925

[2] E. Figueiredo, J.J.S.H.M. Brownjohn, Three decades of statistical pattern recognition paradigm for SHM of bridges, (2022), p. 14759217221075241, DOI: 10.1177/14759217221075241

[3] A.M. D'Altri, V. Sarhosis, G. Milani, J. Rots, S. Cattari, S. Lagomarsino, E. Sacco, A. Tralli, G. Castellazzi, S. de Miranda, Modeling strategies for the computational analysis of unreinforced masonry structures: Review and classification, Archives of Computational Methods in Engineering (2019), pp. 1-33, DOI: 10.1007/s11831-019-09351-x

[4] N. Kassotakis, V.J.S. Sarhosis, Employing non-contact sensing techniques for improving efficiency and automation in numerical modelling of existing masonry structures: A critical literature review, 32 (2021), pp. 1777-1797, DOI: 10.1016/j.istruc.2021.03.111

[5] N. Kassotakis, Efficient and robust numerical modelling of masonry, Newcastle University, 2020. URL: http://theses.ncl.ac.uk/jspui/handle/10443/5336 [Accessed 1st March 2023]

[6] N. Kassotakis, V. Sarhosis, M.-V. Peppa, J.P. Mills, Semi-automated discrete-element modelling of arch structures incorporating SfM photogrammetry, Proceedings of the Institution of Civil Engineers - Engineering History and Heritage (2023), pp. 1-15, DOI: 10.1680/jenhh.21.00007

[7] D. Loverdos, V. Sarhosis, Image2DEM: A geometrical digital twin generator for the detailed structural analysis of existing masonry infrastructure stock, (2023), DOI: 10.1016/j.softx.2023.101323

[8] D. Loverdos, V. Sarhosis, E. Adamopoulos, A. Drougkas, An innovative image processing-based framework for the numerical modelling of cracked masonry structures, Automation in Construction 125 (2021), p. 103633, DOI: 10.1016/j.autcon.2021.103633

[9] T.H. Linh, D.F. Laefer, Octree-based, automatic building facade generation from LiDAR data, Computer-Aided Design 53 (2014), pp. 46-61, DOI: 10.1016/j.cad.2014.03.001

[10] G. Castellazzi, M.A. Altri, G. Bitelli, I. Selvaggi, A. Lambertini, From laser scanning to finite element analysis of complex buildings by using a semi-automatic procedure, Sensors 15 (8) (2015), pp. 18360–18380, DOI: 10.3390/s150818360

[11] N. Kassotakis, V. Sarhosis, B. Riveiro, B. Conde, J. Mills, A. D'Altri, S. Miranda, G. Castellazzi, Three-dimensional discrete element modelling of rubble masonry structures from dense point clouds, Automation in Construction (2020), DOI: 10.1016/j.autcon.2020.103365

[12] B. El Said, D. Ivanov, A.C. Long, S.R. Hallett, Multi-scale modelling of strongly heterogeneous 3D composite structures using spatial Voronoi tessellation, Journal of the Mechanics and Physics of Solids 88 (2016), pp. 50-71, DOI: 10.1016/j.jmps.2015.12.024

[13] B. Pulatsu, S. Kim, E. Erdogmus, P.B. Lourenço, Advanced analysis of masonry retaining walls using mixed discrete–continuum approach, 174 (3) (2021), pp. 302-314, DOI: 10.1680/jgeen.19.00225

[14] B. Pulatsu, S. Gonen, E. Erdogmus, P.B. Lourenço, J.V. Lemos, J. Hazzard, Tensile Fracture Mechanism of Masonry Wallettes Parallel to Bed Joints: A Stochastic Discontinuum Analysis, Modelling 1 (2) (2020), pp. 78-93, DOI: 10.3390/modelling1020006

[15] V. Sarhosis, T. Forgács, J.V. Lemos, Modelling backfill in masonry arch bridges: A DEM approach, in: A. Arêde, C. Costa (Eds.), 9th International Conference on Arch Bridges, Springer International Publishing, Cham, Switzerland, 2019, pp. 178-184

[16] B. Pulatsu, E. Erdogmus, P.B. Lourenço, J.V. Lemos, J. Hazzard, Discontinuum analysis of the fracture mechanism in masonry prisms and wallettes via discrete element method, Meccanica 55 (3) (2020), pp. 505-523, DOI: 10.1007/s11012-020-01133-1

[17] V. Sarhosis, J.V. Lemos, A detailed micro-modelling approach for the structural analysis of masonry assemblages, Computers & Structures 206 (2018), pp. 66-81, DOI: 10.1016/j.compstruc.2018.06.003

[18] P.R. Prakash, B. Pulatsu, P.B. Lourenço, M. Azenha, J.M. Pereira, A meso-scale discrete element method framework to simulate thermo-mechanical failure of concrete subjected to elevated temperatures, Engineering Fracture Mechanics 239 (2020), p. 107269, DOI: 10.1016/j.engfracmech.2020.107269

[19] B. Pulatsu, E. Erdogmus, P.B. Lourenço, J.V. Lemos, K. Tuncay, Numerical modeling of the tension stiffening in reinforced concrete members via discontinuum models, Computational Particle Mechanics 8 (3) (2021), pp. 423-436, DOI: 10.1007/s40571-020-00342-5

[20] R. McNeel, Rhinoceros 3D [Software], 2015

[21] CloudCompare (version 2.1), GPL software, 2019. URL: http://www.cloudcompare.org/ [Accessed 19th January 2020]

[22] M. Kazhdan, H. Hoppe, Screened poisson surface reconstruction, ACM transactions on graphics 32 (3) (2013), pp. 1-13, DOI: 10.1145/2487228.2487237

[23] K. Mamou, F.J.t.I.I.C.o.I.P. Ghorbel, A simple and efficient approach for 3D mesh approximate convex decomposition, (2009), pp. 3501-3504. URL: [Accessed 11th November 2022]

[24] Blender - a 3D modelling and rendering package, 2015. URL: http://www.blender.org [Accessed 19th January 2020]

[25] V-HACD For Blender 4.0, 2022. URL: https://github.com/kmammou/v-hacd [Accessed 19th January 2020]

[26] Matlab, 2019. URL: https://www.mathworks.com/products/matlab.html [Accessed 19th January 2020]

[27] Polytope bounded Voronoi diagram in 2D and 3D, 2023. URL: https://github.com/hyongju/Polytope-bounded-Voronoi-diagram/releases/tag/1.15) [Accessed 1st March 2023]

[28] ITASCA. 3DEC 5.2 – Universal distinct element code manual. Theory and background. Mineapolis., 2019. URL: www.itasca.com [Accessed 19th January 2020]

[29] A.M. D'Altri, F. Messali, J. Rots, G. Castellazzi, S. de Miranda, A damaging block-based model for the analysis of the cyclic behaviour of full-scale masonry structures, Engineering Fracture Mechanics 209 (2019), pp. 423-448, DOI: 10.1016/j.engfracmech.2018.11.046

[30] D. Malomo, R. Pinho, A. Penna, Applied element modelling of the dynamic response of a full-scale clay brick masonry building specimen with flexible diaphragms, International Journal of Architectural Heritage (2019), p. 1616004, DOI: 10.1080/15583058.2019.1616004

[31] J.V. Lemos, Discrete element modeling of masonry structures, International Journal of Architectural Heritage 1 (2) (2007), pp. 190-213, DOI: 10.1080/15583050601176868

[32] A. Shabani, M. Feyzabadi, M. Kioumarsi, Model updating of a masonry tower based on operational modal analysis: The role of soil-structure interaction, Case Studies in Construction Materials 16 (2022), p. e00957, DOI: 10.1016/j.cscm.2022.e00957

[33] V. Sarhosis, S.W. Garrity, Y. Sheng, Influence of brick-mortar interface on the mechanical behaviour of low bond strength masonry brickwork lintels, Engineering Structures 88 (2015), pp. 1-11, DOI: 10.1016/j.engstruct.2014.12.014

[34] V. Sarhosis, T. Forgacs, J. Lemos, Stochastic strength prediction of masonry structures: a methodological approach or a way forward?, RILEM Technical Letters 4 (0) (2020), pp. 122-129, DOI: 10.21809/rilemtechlett.2019.100

[35] S. Casolo, Modelling in-plane micro-structure of masonry walls by rigid elements, International Journal of Solids and Structures 41 (2004), pp. 3625-3641, DOI: 10.1016/j.ijsolstr.2004.02.002

[36] F. Vanin, D. Zaganelli, A. Penna, K. Beyer, Estimates for the stiffness, strength and drift capacity of stone masonry walls based on 123 quasi-static cyclic tests reported in the literature, Bulletin of Earthquake Engineering 15 (12) (2017), pp. 5435-5479, DOI: 10.1007/s10518-017-0188-5

[37] O.E.C. Prizeman, V. Sarhosis, A.M. D'Alri, C.J. Whitman, G. Muratore, Modelling from the past: The leaning southwest tower of caerphilly castle 1539-2015, ISPRS Annals of Photogrammetry, Remote Sensing and Spatial Information Sciences, Vol. IV-2/W2, Ottawa, Canada, 2017, pp. 221-227

[38] D. Renn, Caerphilly Castle, Cardiff, UK, 1st ed., Cadw, 2002. ISBN: 978-1-85760-082-7.

[39] G. Castellazzi, A.M. D'Altri, S. de Miranda, F. Ubertini, An innovative numerical modeling strategy for the structural analysis of historical monumental buildings, Engineering Structures 132 (2017), pp. 229-248, DOI: 10.1016/j.engstruct.2016.11.032

[40] A.M. D'Altri, G. Milani, S. Miranda, G. Castellazzi, V. Sarhosis, Stability analysis of leaning historic masonry structures, Automation in Construction 92 (2018), pp. 199–213, DOI: 10.1016/j.autcon.2018.04.003

[41] M. Dejong, Seismic assessment strategies for masonry structures, Ph.D., Department of Architecture, Massachusetts Institute of Technology, 2009. URL: https://dspace.mit.edu/handle/1721.1/49538 [Accessed 19th January 2020]

[42] S. Acikgoz, M.J. DeJong, K. Soga, Sensing dynamic displacements in masonry rail bridges using 2D digital image correlation, Structural Control and Health Monitoring 25 (8) (2018), DOI: 10.1002/stc.2187

[43] S. Cocking, D. Thompson, M. DeJong, Comparative Evaluation of Monitoring Technologies for a Historic Skewed Masonry Arch Railway Bridge, Structural Integrity, Vol. 11, 2020, pp. 439-446

[44] K. Faulkner, F. Huseynov, J. Brownjohn, Y. Xu, Deformation Monitoring of a Simply Supported Railway Bridge under Varying Dynamic Loads, (2018), pp. 1484-1491, DOI: 10.1201/9781315189390-202